Compact laser radar and three-dimensional camera

Antonio Medina, Francisco Gayá, and Francisco del Pozo

University of Madrid, School of Electrical and Telecommunication Engineering (ETSIT), Department of Photonic Technology, Bioengineering and Telemedicine Group (GBT) Laboratory, Madrid 28003, Spain

Received April 14, 2005; revised August 5, 2005; accepted August 18, 2005; posted September 22, 2005 (Doc. ID 61360)

A novel three-dimensional (3D) camera is capable of providing high-precision 3D images in real time. The camera uses a diode laser to illuminate the scene, a shuttered solid-state charge-coupled device (CCD) sensor, and a simple phase detection technique based on the sensor shutter. The amplitude of the reflected signal carries the luminance information, while the phase of the signal carries range information. The system output is coded as a video signal. This camera offers significant advantages over existing technology. The precision in range is dependent only on phase shift and laser power and theoretically is far superior to existing time-of-flight laser radar systems. Other advantages are reduced size and simplicity and compact and inexpensive construction. We built a prototype that produced high-resolution images in range the (z) and $x-y$.

OCIS codes: 040.0040, 110.0110, 120.0120, 140.0410, 150.0150, 280.0280.

1. INTRODUCTION

The problem of collecting three-dimensional (3D) information, in general and as it applies to optical images, has been explored by many investigators because it applies to multiple fields and has many applications.

One classical approach, stereo image processing, is well developed, but is too slow and computationally intensive for many applications. A fundamental limitation of stereo ranging is that range resolution decreases with distance.[1]

Laser radar (ladar) systems[2,3] measure the time of flight, the time it takes the illuminating energy (laser light) to reach the target and reflect back to the sensor. Since the speed of light is very high, these systems are limited by their ability to discriminate very short energy pulses and to form an image. A way to alleviate such a limitation is to use modulated light so that a phase measurement, rather than a time measurement, is made. If a modulated laser beam scans a scene and an appropriate sensor detects the reflected energy, an image is obtained. The amplitude of the sensor output signal corresponds to the reflectivity of the scene and the phase of the modulation is linearly related to range. The main limitation of this system is that it requires cumbersome mechanical scanners rather than conventional imaging optics. The need to scan the scene with a laser beam and the mechanical complexity and reliability of the scanner optics result in slow, low-resolution systems.[4,5] Methods that do not require scanners have been devised, but they lack imaging capabilities[6] or require specially designed sensors.[7]

Range detection is currently used in commercial, scientific, and military applications. Most applications require speed and accuracy. Some systems deliver accurate results that are obtained by non-real-time processing of images after the acquisition is completed. The time it takes to obtain such results can be shortened, but only at the expense of sophistication, which in turn drives the complexity, bulk, and price upwards.

Numerous efforts have been made to create 3D imaging systems using time-of-flight principles, but to date none is capable of using a conventional sensor. The concept of using a shutter as a demodulator for a ladar optical signal was first devised and reported by Medina.[8] Since then there have been attempts to implement the concept, but all relied on external or specially designed shutters.[7,9–11] We report the implementation of this concept using a conventional CCD. The breakthrough advantage of this technique is its unsurpassed simplicity and range precision.

Our system overcomes the limitations of existing time-of-flight and modulated systems. We use a pulsed diode laser to illuminate the scene, a CCD camera, and a novel phase detection technique. This system is a 3D video camera with video signals that carry the luminance information and the range information in real time. We refer to the camera as 3D in a general sense. The camera used determines the $x-y$ resolution. High $x-y$ resolution can be obtained by utilizing high-resolution camera sensors. For each pixel, the system outputs luminance and range information as a function of time. The luminance information contains object identification information, as in other systems. The range information acquired by this ladar system can be easily processed to derive the shape, velocity, and acceleration of an object in real time. The range precision of the proposed system is dependent only on phase shift and the power of the laser illuminator. Therefore the range precision is independent of distance and of the spatial resolution of the camera if a laser of appropriate power is used. Each picture element has a luminance value plus a range value.

The ladar technique that our group developed outperforms results reported by other groups. The direct shut-

tering of the CCD not only increases the signal-to-noise ratio, but also simplifies the phase detection enormously and makes the whole system practical. The range precision is considerably reduced when the illuminator power is less than optimal due to quantum noise, as shown in Subsection 3.B. The breakthrough advantage of our system is that the laser pulse can be relatively long, reducing the bandwidth requirement, and it permits use of a conventional CCD or complementary metal-oxide semiconductor (CMOS) sensor.

2. METHODS

A. Principle of Operation

We built a system as schematically depicted in Fig. 1. A pulsed laser illuminates a scene that is imaged by a shuttered CCD video camera. The optical signal at the aperture of the camera contains the two-dimensional reflectivity information of the scene plus the range information as a spatial phase modulation of the train of laser pulses. The crucial parts of the system are the pulsed laser and the shuttered image sensor. We used a novel phase detection scheme to extract the phase directly from an interline-transfer CCD that is effectively turned on during the reception of the laser pulses. We built our prototype using 80 OSRAM SPL PL90-3 laser diodes and a PULNiX camera equipped with an interline-transfer-type CCD, Kodak model KAI-311M. The diodes emitted simultaneous pulses of light at a wavelength of 905 nm and a

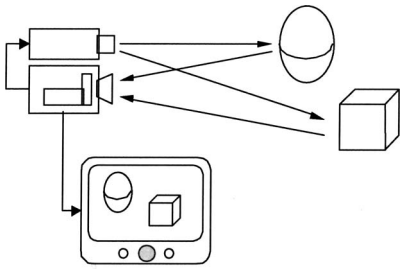

Fig. 1. Block diagram of the 3D camera. Light pulse (arrows) emitted by the laser (top left) is recorded in part by the shuttered camera (below laser) after reflecting off the scene objects (right); the part recorded is related to the depth of the objects and is displayed in the monitor (bottom) in several ways.

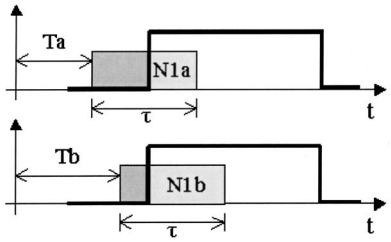

Fig. 2. Principle of detection of phase. Light pulse of duration τ (shaded) reflected by a near object arrives to the camera at a time Ta shorter than the time of arrival of light reflected by the far object Tb. The photons recorded in the pixels corresponding to the near object (light-shaded $N1a$) are less than for the far object (light-shaded $N1b$) when a shutter allows light at the time indicated by the thick line. The time axis is denoted as t. The vertical axis is the light recorded as a photoelectron count. The dark-shaded area represents the light rejected, referred to as $N2$ in the text.

20 ns duration that directly illuminated a field of 25 by 25 deg. We chose the focal length of the camera lens so that its field of view matched the illuminating field. We also designed and built digital electronics comprising the controller for the laser and the CCD camera. The system uses commercially available components. We display the range images on a standard monitor using gray or color coding for the range.

B. Phase Detection

The direct detection of the phase of a reflected signal by a CCD sensor is the key and novel feature of the 3D camera that enables the measurement of range with reduced peak power. Figure 2 illustrates the arrangement of laser pulses and shutter timing for phase detection and the output of a pixel of the CCD camera.

The laser source transmits pulses of light (Fig. 2 depicts one such pulse, as detected in one pixel photosite of the CCD). Pulses are emitted continuously and periodically; the period is a horizontal video period (for a repetition rate of ~15 kHz). The pulse width (τ) is shorter than the horizontal period. Two considerations are taken into account in the design. For a given repetition rate, the smaller τ is, the greater the peak power must be. Most importantly, as will be seen in Section 3, τ is related to the range of interest (R) and must be chosen accordingly. If R equals 1 km, then τ should equal 6.6 μs for maximum range precision. If the range of interest is a few meters, then τ should equal a few nanoseconds (6.6 ns/m). A diode laser was used because it is well suited for the pulse lengths required. They are also capable of providing the required average power.

As objects in the scene reflect the light pulses emitted by the laser source, light pulses are received at the camera location, but are delayed with respect to pulses at the source because of the finite velocity of travel of light, as indicated by Ta and Tb in Fig. 2.

The shutter of the camera opens and closes periodically at the same frequency as the laser pulses and at the time indicated by the thick line in Fig. 2. The result of the shuttering is, in effect, the product of two functions: the train of delayed pulses and the shutter wave response. The product of a phase-modulated signal (train pulses) and a reference signal of the same frequency (shutter wave) results in a synchronous detection of phase.

Shuttering of the CCD camera is achieved by dumping the photosite charge to the CCD substrate while the pulse has not fully arrived to the CCD and then transferring the photoelectrons ($N1$) from their photosites to the vertical transport registers. $N1$ is therefore the collected portion of the received light pulse and $N2$ is the portion of the light pulse rejected by the shutter. The time needed to transfer the charge is very short, of the order of 30 ns. The 3D camera reads out a regular (nonshuttered) image N ($N=N1+N2$) as the subsequent frame. In this way, the charge corresponding to portions $N1$ and N are read as successive frames. It is also possible to obtain $N1$ and $N2$ with a single pulse, but with a commercial CCD the laser pulses would have to operate at the CCD's frame rate instead of the horizontal line rate.

We use a progressive (noninterlaced) scan camera. For each range reading, the camera outputs two frames con-

taining the fore portion and the total pulse energy of the pulse ($N1$ and N, respectively). We refer to these frames as the $N1$ and N frames. The $N1$ frame contains $N1$ photoelectrons in a representative pixel while the N frame contains $N=N1+N2$.

The ratio (pixel by pixel) of $N1$ and N frame registers results in a range register containing phase information. Depending on the distance to the picture element, the phase measurement will vary between the values 0 and 1 for each pixel. The actual range is obtained by mapping (scaling) the range register according to a calculated or calibrated factor. Our camera includes a background frame acquisition and subtraction as part of the calibration.

3. RESULTS

A. System Analysis and Performance

An analysis of the theoretical performance of the 3D camera, and of its performance accounting for practical limitations, follows below together with actual performance of our prototype.

To model the proposed system, we develop in this subsection an expression for the system response, which incorporates realistic approximations or actual performance measured from system components. The power transmitted by the laser at time t is given by $p_e(t)$. Then, at the focal plane in front of the ith CCD cell, the power received at time t is given by

$$p(t) = \rho p_e(t - T), \tag{1}$$

where T is the pulse time of flight, which is a function of the range to the target and is the quantity we wish to estimate, and ρ is a coefficient combining the unknown surface reflection and the attenuation loss. The CCD collected charge from the ith pixel is the power received multiplied by the shutter response and integrated over time:

$$N1 = \int_{-\infty}^{\infty} p(t)W(t)\mathrm{d}t. \tag{2}$$

In this expression $W(t)$ is the CCD shutter response. Notice that $N1$ is a function of range, and it is the temporal convolution of the pulse waveform and the shutter response. We shall assume the shutter response to be given by

$$W(t) = \begin{cases} \Gamma & \text{if } t \leq T_R \\ 1 + (\Gamma - 1)\exp(-\alpha(t - T_R)), & \text{if } t > T_R \end{cases}. \tag{3}$$

In this expression T_R represents the time when the shutter starts to open, while α, the shutter time constant, allows for the fact that shuttering is not instantaneous, but the transmitted intensity progresses exponentially. Typically, the shuttering time $1/\alpha$ is of the order of 30 ns for our shutter. Finally, Γ allows for the fact that a residual amount of light may be transmitted due to electron leakage from the photosites. In our camera, Γ is less than 2%.

We estimate the round-trip time and the reflection coefficient by combining two measurements. The first measurement is the integrated signal from a shuttered CCD array. The second measurement, which is used to calibrate out the surface reflectivity, is obtained by integrating over the whole return pulse. This is accomplished as explained above. Writing the first measurement as $N1$ and the second one as N, we form the quantity that gives as the range

$$r = \frac{N - N1}{N} = 1 - \frac{N1}{N} \Rightarrow 0 \leq r \leq 1. \tag{4}$$

The quantity r, which we will call the normalized range, is independent of the surface reflection coefficient and depends only on the travel time, which is unknown, and the shutter time, which is known. In addition, because we use the integrated return power, this is a monotonically decreasing function of $(T_R - T)$. It approaches 0 and 1 asymptotically as T approaches $(\pm)$ infinity (see Fig. 3). Since the normalized range is a monotonically decreasing function, it can be inverted to obtain an estimate of the arrival time for an arbitrary pulse shape. This process will be clarified with the following analysis for a Gaussian pulse shape. The actual laser-pulse shape is close to this shape.

Let the pulse shape be given by

$$p_e(t) = p_o \exp\left(\frac{-t^2}{2\tau'^2}\right), \tag{5}$$

where p_o is the maximum height of the pulse and τ' is an effective pulse length, equal to the pulse full width at half-height multiplied by 0.425. The integrated charge can be calculated to be

$$N1 = \rho p_o \left[\int_{-\infty}^{T_R} \exp\left(\frac{-(t-T)^2}{2\tau'^2}\right) * \Gamma \mathrm{d}t + \int_{T_R}^{\infty} \exp\left(\frac{-(t-T)^2}{2\tau'^2}\right)(1 + (\Gamma - 1)\exp(-\alpha(t - R)))\mathrm{d}t \right]. \tag{6}$$

Expanding the integrals we arrive at

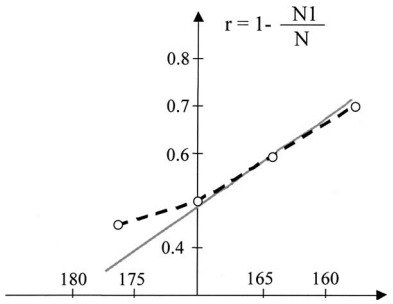

Fig. 3. Theoretical range curve for a Gaussian pulse (solid line). Dotted curve is the measured range from the actual camera. The horizontal axis denotes delay T in nanoseconds.

$$N1 = \rho p_o \tau' \sqrt{\frac{\pi}{2}}\left[\left[\Gamma + 1 + (1-\Gamma)\mathrm{erf}\left(\frac{t_o}{\sqrt{2}\tau'}\right) - \exp\left(\frac{\alpha^2\tau'^2}{2}\right)\exp(-\alpha t_o)\left(1 + \mathrm{erf}\left(\frac{t_o}{\sqrt{2}\tau'} - \frac{\alpha\tau'}{\sqrt{2}}\right)\right)\right]\right], \tag{7}$$

where $\mathrm{erf}(x)$ is the error function of x, defined as

$$\mathrm{erf}(x) = \frac{2}{\sqrt{\pi}}\int_0^x \exp(-t^2)\mathrm{d}t. \tag{8}$$

The value N is a particular case of $N1$ where the delay is very large and all the pulse is received; therefore, for N, $W(t)=1$ and

$$N = \int_{-\infty}^{\infty} p(t)\mathrm{d}t, \tag{9}$$

$$N = k\rho p_o \int_{-\infty}^{\infty} \exp\left(\frac{-(t-T)^2}{2\tau'^2}\right)\mathrm{d}t = k\rho p_o \sqrt{2\pi}\tau'. \tag{10}$$

The normalized range is

$$r = 1 - \frac{1}{2}\left[\Gamma + 1 + (1-\Gamma)\left[\mathrm{erf}\left(\frac{t_o}{\sqrt{2}\tau'}\right) - \exp\left(\frac{\alpha^2\tau'^2}{2}\right) \times \exp(-\alpha t_o)\left(1 + \mathrm{erf}\left(\frac{t_o}{\sqrt{2}\tau'} - \frac{\alpha\tau'}{\sqrt{2}}\right)\right)\right]\right]. \tag{11}$$

This curve cannot be solved analytically, but may be solved numerically, or by means of look-up tables and interpolation. A plot of this curve is presented in Fig. 3 together with actual values measured from our prototype.

A range curve was also obtained repeating the process with rectangular and triangular pulse shapes. The actual laser-pulse shape is closer to the Gaussian, but the other shapes did not produce different results.

The normalized range curve is dependent on the shutter speed. It can be shown that if the curve in Fig. 3 is plotted for a shutter faster than 30 ns, the slope of the curve increases and, correspondingly, the range precision.

B. Range Precision

We wish to evaluate the relative accuracy to which the range to a single hard target can be registered within a given pixel under optimal or ideal conditions.

The ultimate limit to the precision in range is imposed by quantum noise. For an ideal camera with square pulsed illumination and fast shutter, the range is given by the following equation (see Fig. 2):

$$z = \frac{R}{2N}(N2 - N1) + \frac{R}{2}, \tag{12}$$

where R is the range of interest that equals $c\tau/2$, $N1$ is the photoelectrons generated in a pixel for the N_1 frame, $N2$ is the photoelectrons rejected by the shutter, and $N = N1 + N2$. The error in range z is related to the error made in measuring $N1$ (and $N2$).

We know that the standard deviation σ of the distribution of N photons and electrons collected in a time interval is

$$\sigma_{N1} = \sqrt{N1} \quad \text{for } N1, \tag{13}$$

$$\sigma_{N2} = \sqrt{N2} \quad \text{for } N2. \tag{14}$$

The standard deviation of a quantity that is the difference of measured quantities is equal to the square root of the sum of the squares of the standard deviations of the measured quantities:

$$\sigma_{N2-N1} = \sqrt{{\sigma_{N1}}^2 + {\sigma_{N2}}^2} = \sqrt{N1 + N2} = \sqrt{N}. \tag{15}$$

Assuming that the CCD pixel wells are filled with electrons to their maximum capacity,

$$\sigma_z = \frac{R}{2N}\sigma_{N2-N1} = \frac{R}{2N}\sqrt{N}. \tag{16}$$

If we take the maximum well capacity of a CCD equal to 10^6 electrons,

$$\frac{\sigma_z}{R} = \frac{\sqrt{N}}{2N} = \frac{\sqrt{10^6}}{2\times 10^6} = 5\times 10^{-4}. \tag{17}$$

The precision in range (range uncertainty) due to quantum noise is therefore approximately 1 part in two thousand. For a range of interest of 20 m, the precision is $20/2000 = 0.01$ m.

Our CCD has a well capacity of 50,000 electrons, Therefore the range precision of our prototype is 2.2 parts in one thousand. Since our range of interest is 2 m, the theoretical range precision is 4.4 mm. Of course, practical limitations reduce the theoretical limit. In particular the nonideal shutter and laser pulse and electrical noise did reduce the precision by almost an order of magnitude as discussed below.

C. Power of the Laser

The radiant intensity levels needed for operation of the ladar camera are of the same order of magnitude as in a conventional imaging system with artificial illumination. We will see that, to achieve maximum precision in the range, an optimum intensity must be delivered to the scene.

If we assume the scene to be a Lambertian reflector, all the energy from the source will be reflected and radiated over a hemisphere (2π rad) with uniform radiance. Only energy falling in the solid angle subtended by the camera aperture will be collected.

The fraction of source energy collected by the camera is

$$\frac{\Omega}{2\pi} = \frac{\pi D^2/4r^2}{2\pi} = \frac{1}{8}\left(\frac{D}{r}\right)^2, \tag{18}$$

where Ω is the solid angle subtended by the camera lens, D is the diameter of the camera lens, and r is the distance to the scene.

The energy that must be radiated per pixel is given by

$$E = \frac{Nh\nu}{\frac{1}{8}\left(\frac{D}{r}\right)^2 \eta a \delta} \text{ (joules)}, \tag{19}$$

where N is the number of photoelectrons required per pixel, η is the sensor efficiency, a is the reflectivity, δ is the camera transmission losses, and $h\nu = 2.5 \times 10^{-19}$ J/photon.

The average power of the illuminating source is

$$P = \frac{Enm}{T} \text{ (watts)}, \tag{20}$$

where n is the number of pixels in each row, m is the number of pixels in each column, and T is the integration time.

For our prototype unit using a Kodak KAI-311M CCD, we have $D = 5 \times 10^{-2}$ m, $r = 10$ m (furthest range or worst case), $N = 50{,}000$ electrons (maximum capacity), $\eta = 0.03$ (quantum efficiency at 905 nm), $a = 0.2$, $\delta = 0.5$, $n = 484$, $m = 648$, $T = 1/60$ s, and $P = 8Nh\nu\text{nm}/(D/r)2\eta a \delta T = 1.5$ W.

The power increases with range (square law), e.g., for a range of 100 m, the power needed is 150 W. Increased x–y resolution also calls for increased power. Notice that the range and the integration time can be selected electronically, adding versatility to the system.

The values calculated above are optimum values for greatest range precision. Operation at greater ranges will reduce the precision. Even if power is increased proportionally, at very large ranges in the atmosphere, volume backscatter will be an added limiting factor.

D. Ambient Light Rejection and Eye Safety

The operation of a ladar during the day places the laser illumination of the target in competition with solar or other types of target illumination. There are several approaches to substantially eliminate this problem.

One solution is to place a narrow bandpass filter in front of the camera lens that passes the laser light but blocks the solar spectral emission outside the band of the filter. Another approach is to limit the solar light with a shutter to exactly the time when the laser return is received. In a pulsed system, like the one proposed, the ambient light rejected this way is very large, as large as the pulse duty cycle. This method, however, is ineffective in sinusoidally modulated systems and cw systems in general. A third approach is to eliminate or at least reduce the competition with the Sun by operating in separate bands. This requires illuminating the target in the ultraviolet (wavelengths shorter than 300 nm), outside the solar spectrum on the Earth's surface. This method will require a special, backilluminated CCD, sensitive to the ultraviolet band.

The 3D camera proposed here has a built-in shutter that makes the second approach practical and easy to build into the system. Use of a filter, in which the band is matched to the laser band, is a nonexclusive approach that can always be used to supplement the time rejection method.

The design we built is eye safe. A number of factors determine the eye safety of the system, such as the wavelength, power, and pulse characteristics of the laser of choice. The fact that this system operates with a divergent laser beam, rather than a collimated beam, is of crucial importance and makes possible eye safety in visible and near-visible wavelengths for the power required for imaging at several meters.

4. PERFORMANCE TESTS AND CONCLUSION

We obtained 3D information with a standard video camera and simple equipment; we relied on the built-in shutter capabilities of the camera CCD for 3D recording. A toy horse and a rabbit were placed on a table at a distance of 2.5 m, the background is a wall at ~3.5 m, and the size of the rabbit head is 0.15 m. We displayed the 3D information as a color image map (see Fig. 4). The raw range data are mapped into color according to the calibration scale in Fig. 4. Notice that the range of interest in this case is 2.5–3.5 m and that precision of a few centimeters is readily attainable. For example, the rabbit depth within the ear is resolved. The precision achieved with our prototype camera is close to an order or magnitude lower than the theoretical maximum of 4.4 mm. The reduced precision is due to the nonidealities of the camera, mainly the reduced speed of the shutter and the pulse shape and width. This paper demonstrates that centimetric precision can be readily achieved with this camera using standard sensors, and also predicts millimetric precision if the

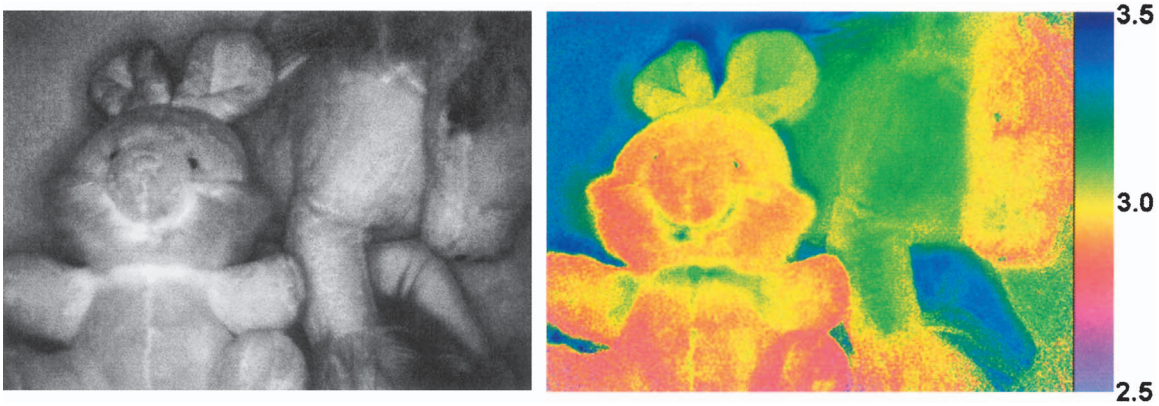

Fig. 4. Sample reflectivity image (N) and range image ($N1/N$) coded and calibrated with a color scale where the numbers indicate distance from the camera in meters.

ideal conditions are met. The image in Fig. 4, and its raw data, can be downloaded from our website.[12] We also processed the 3D image to generate arbitrary views and stereo pairs. See Ref. 12 for stereo pair generation from 3D camera data. The camera is particularly well suited to provide 3D vision to a machine because the range and luminance data are obtained in perfect registration and in real time.

ACKNOWLEDGMENTS

This work was supported in part by the Spanish Ministry of Science and the National Aeronautic and Space Administration. We make special mention to the following scientists and engineers that made this camera possible: Francisco Redondo, Juan Ruiz, Daniel Diner, and David Martin.

Corresponding author A. Medina's e-mail address is amedina@gbt.tfo.upm.es.

REFERENCES

1. O. Faugeras, *Three Dimensional Computer Vision: A Geometric Viewpoint* (MIT Press, 1993).
2. R. A. Lewis and A. R. Johnston, "A scanning laser rangefinder for a robotic vehicle," in *Proceedings of the Fifth International Joint Conference on Artificial Intelligence*, W. Kaufmann, ed. (Morgan Kaufmann, 1977), pp. 762–768.
3. H. Ailisto, V. Heikkinen, R. Mitikka, R. Miyllyia, J. Kostamovaara, A. Mantiniemi, and M. Koskinen, "Scannerless imaging pulsed-laser range finding," J. Opt. **4**, S337–S346 (2002).
4. D. Nitzan, A. E. Brain, and R. O. Duda, "The measurement and use of registered reflectance and range data in scene analysis," Proc. IEEE **65**, 206–220 (1977).
5. B. Stann, W. Ruff, and Z. Sztankay, "Intensity-modulated diode laser radar using frequency-modulation/continuous-wave ranging techniques," Opt. Eng. (Bellingham) **35**, 3270–3278 (1996).
6. N. Takeuchi, H. Baba, K. Sakurai, and T. Ueno, "Diode-laser random modulation cw lidar," Appl. Opt. **25**, 63–67 (1986).
7. R. Lange and P. Seitz, "Solid-state, time-of-flight range camera," IEEE J. Quantum Electron. **37**, 390–397 (2001).
8. A. Medina, "Three dimensional camera and range finder," U.S. patent 5,081,530 (Jan. 14, 1992).
9. J. Anthes, D. Garcia, and D. Dressendorfer, "Non-scanned ladar imaging and applications," in *Applied Laser Radar Technology*, G. W. Kamerman and W. E. Keicher, eds., Proc. SPIE **1936**, 11–22 (1993).
10. R. Miyagawa and T. Kanade, "CCD-based range-finding sensor," IEEE Trans. Electron Devices **44**, 1648–1652 (1997).
11. L. Viarani, D. Stoppa, L. Gonzo, M. Gottardi, and A. Simoni, "A CMOS smart pixel for active 3D vision applications," IEEE Sens. J. **4**, 145–152 (2004).
12. A. Medina and D. Martin, "3D camera," http://www.gbt.tfo.upm.es/investigacion/3D_i.html (2005).